

Experimental characterization of pairwise correlations from triple quantum correlated beams generated by cascaded four-wave mixing processes

Wei Wang, Leiming Cao, Yanbo Lou, Jinjian Du, and Jietai Jing

Citation: *Appl. Phys. Lett.* **112**, 034101 (2018); doi: 10.1063/1.5000772

View online: <https://doi.org/10.1063/1.5000772>

View Table of Contents: <http://aip.scitation.org/toc/apl/112/3>

Published by the [American Institute of Physics](#)

Articles you may be interested in

[High breakdown electric field in \$\beta\$ -Ga₂O₃/graphene vertical barristor heterostructure](#)

Applied Physics Letters **112**, 032101 (2018); 10.1063/1.5002138

[Single photon sources in 4H-SiC metal-oxide-semiconductor field-effect transistors](#)

Applied Physics Letters **112**, 031105 (2018); 10.1063/1.4994241

[Enhancement of wind energy harvesting by interaction between vortex-induced vibration and galloping](#)

Applied Physics Letters **112**, 033901 (2018); 10.1063/1.5007121

[Experimental observation of multi-spatial-mode quantum correlations in four-wave mixing with a conical pump and a conical probe](#)

Applied Physics Letters **110**, 241103 (2017); 10.1063/1.4985706

[Lithium ion intercalation in thin crystals of hexagonal TaSe₂ gated by a polymer electrolyte](#)

Applied Physics Letters **112**, 023502 (2018); 10.1063/1.5008623

[Resonant enhancement of accelerating gradient with silicon dual-grating structure for dielectric laser acceleration of subrelativistic electrons](#)

Applied Physics Letters **112**, 034102 (2018); 10.1063/1.5010144

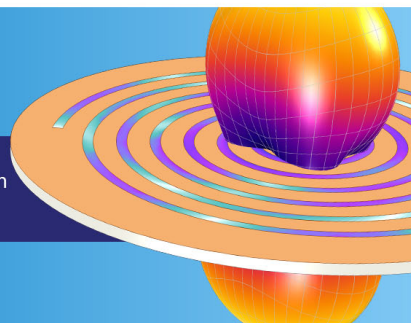
**COMSOL
CONFERENCE
2018 BOSTON**

Discover the power of multiphysics simulation.

COMSOL

OCTOBER 3-5
Boston Marriott Newton

Register Now ▶



Experimental characterization of pairwise correlations from triple quantum correlated beams generated by cascaded four-wave mixing processes

Wei Wang,¹ Leiming Cao,¹ Yanbo Lou,¹ Jinjian Du,¹ and Jietai Jing^{1,2,3,a)}

¹State Key Laboratory of Precision Spectroscopy, East China Normal University, Shanghai 200062, China

²Department of Physics, Zhejiang University, Hangzhou 310027, China

³Collaborative Innovation Center of Extreme Optics, Shanxi University, Taiyuan, Shanxi 030006, China

(Received 18 August 2017; accepted 29 December 2017; published online 16 January 2018)

We theoretically and experimentally characterize the performance of the pairwise correlations from triple quantum correlated beams based on the cascaded four-wave mixing (FWM) processes. The pairwise correlations between any two of the beams are theoretically calculated and experimentally measured. The experimental and theoretical results are in good agreement. We find that two of the three pairwise correlations can be in the quantum regime. The other pairwise correlation is always in the classical regime. In addition, we also measure the triple-beam correlation which is always in the quantum regime. Such unbalanced and controllable pairwise correlation structures may be taken as advantages in practical quantum communications, for example, hierarchical quantum secret sharing. Our results also open the way for the classification and application of quantum states generated from the cascaded FWM processes. *Published by AIP Publishing.*

<https://doi.org/10.1063/1.5000772>

Multipartite quantum correlation is of great significance for fundamental research^{1,2} and the future development of quantum information technology.^{3,4} This development will need strong quantum correlation for the purpose of high fidelity quantum communications.⁵ This development will also require an efficient quantum interface between multipartite quantum light sources and atomic ensembles, which makes it necessary to implement multipartite quantum light sources that match the atomic transitions.⁶ The multipartite correlation shows the quantum property of the whole system, while the pairwise correlations (PCs) can be used to better understand the internal structure of a system. They provide a greatly simplified description of complex systems and allow for the analysis of what might otherwise be intractable problems.^{7,8} The relationship between quantum correlation of multiple quantum correlated beams and multi-beam PC remains an open problem.^{9–14}

In recent years, four-wave mixing (FWM) processes based on atomic ground state coherence in atomic vapor have been demonstrated to be good candidates for produce quantum-correlated twin beams^{15–21} and therefore have found many interesting applications.^{22–28} Most importantly, the frequencies of the generated beams naturally match with the atomic transitions of atomic ensembles due to the fact that the beams are directly generated from the atomic ensembles. Such natural matching is perfect for the future development of quantum information technology in terms of the efficient quantum interface mentioned above.⁶ It is worth noting that the quantum correlation has also been observed recently using the multi-wave mixing process in atomic ensembles²⁹ or rare-earth-doped crystals.³⁰ Recently, our group theoretically proposed and experimentally demonstrated a method to generate multiple spatially multimode quantum correlated beams based

on FWM processes in hot Rb vapor.³¹ Under that experimental condition, there does not exist any quantum correlation between any two of the triple-beams. In other words, there is no PC with quantum correlation which has been shown in our previous work. Therefore, the dependence of the PCs on the system operating condition of the cascaded FWM processes is very interesting and worth studying. In this letter, in order to systematically study the relationship between the triple-beam quantum correlation and PCs, we carry out both the theoretical and experimental studies. We use the degree of squeezing (DS) to characterize the degree of quantum correlation of the triple-beams and PCs and study the dependence of the DS on the gain of the FWM process in four cases.

Our scheme uses two parametric amplifiers (PAs) to generate the triple quantum correlation beams as shown in Fig. 1(a). A coherent probe beam (Pr_0) is seeded into a PA (PA_1), with a gain of G_1 , where it crosses with a pump beam (P_1). The output probe beam is amplified (Pr_1), and a conjugate beam (C_1) is simultaneously generated. We then pick out one of the [assume Pr_1 as shown in Fig. 1(a)] twin beams and use it to seed the second identical PA (PA_2). This beam is amplified (Pr_2) with a gain of G_2 , and at the same time, a new conjugate beam (C_2) is generated. The advantage of our system is the phase insensitivity that makes it possible to easily extend our system to a large number of modes, as it does not require relative phase stability between all the parametric amplification processes. In order to better fit the experimental results, we take into account the experimental imperfections, such as the transmission loss and detection loss. The total detection efficiency of the three detectors is denoted by η . The transmission efficiency between the two cells is η_{int} .

Our corresponding detailed experimental layout is shown in Fig. 1(b). Two identical FWM processes are used as the two PAs for generating quantum correlated triple-beams. An external cavity diode laser (ECDL) is used as our main laser. The ECDL has a linewidth of 100 kHz tuned about 0.8 GHz to

^{a)}Author to whom correspondence should be addressed: jtjing@phy.ecnu.edu.cn

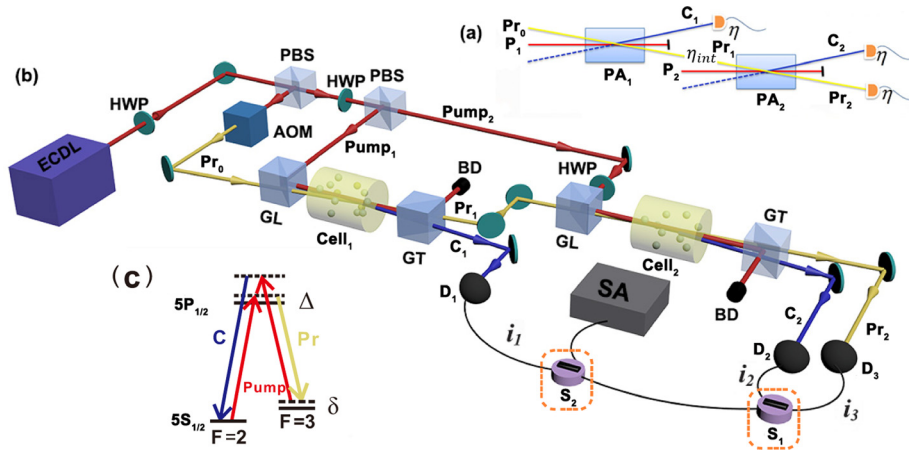


FIG. 1. Experimental layout for generating and detecting quantum correlated triple-beams. (a) Cascaded FWM Process. (b) Experimental setup. ECDL, external cavity diode laser; HWP, half-wave plate; PBS, polarization beam splitter; AOM, acousto-optic modulator; GL, Glan-Laser polarizer; GT, Glan-Thompson polarizer; BD, beam dump; Cell_i, rubidium vapor cell; D_i, photodetectors; S_i, subtractors; SA, spectrum analyzer; Pr₀, initial probe beam; Pr₁ and Pr₂, first and second probe beams; and C₁ and C₂, first and second conjugate beams. (c) Double $-\lambda$ scheme in the D1 line of ^{85}Rb . Pump: pump beams; Pr: probe beam; C: conjugate beam; Δ : one-photon detuning; δ : two-photon detuning.

the blue of the ^{85}Rb $5S_{1/2}, F=2 \rightarrow 5P_{1/2}$ transition, which is called one-photon detuning (Δ). The total output power of the ECDL is around 3 W. A polarizing beam splitter (PBS) is used to split the beam into two. One of the beams is used for the two pump beams of the two FWM processes. The other beam is double passed through an acousto-optic modulator (AOM). In this way, a much weaker probe beam 3.04 GHz red detuned to the pump is derived, which is also 4 MHz detuned from the ^{85}Rb ground-state hyperfine splitting of 3.036 GHz, called two-photon detuning (δ). Figure 1(c) shows the double- Λ FWM configuration of ^{85}Rb vapor.

The two identical ^{85}Rb vapor cells are 12 mm long and temperature stabilized at around 110 °C. They are illuminated by intense vertically polarized pump beams (both Pump₁ and Pump₂ are about 280 mW) with beam waists of about $550\ \mu\text{W}$. Two horizontally polarized probe beams (Pr₀ and Pr₁) are crossed with beams Pump₁ and Pump₂ at the same angle of about 6 mrad at the center of cell₁ and cell₂, respectively. The beam Pr₀ has a power of $20\ \mu\text{W}$ and a beam waist $280\ \mu\text{m}$. The gains of these two vapor cells are G_1 and G_2 , respectively. Based on these settings, the initial probe beam (Pr₀) is amplified twice, becoming Pr₂. At the same time, two new conjugate beams (C₁ and C₂) are generated. As shown in Ref. 31, the intensity-difference noise of these triple-beams (C₁, C₂, and Pr₂) is squeezed compared to the corresponding shot noise limit (SNL) by a factor of $1/(2G_1G_2 - 1)$. These triple-beams are sent to three photodiodes (D₁, D₂, and D₃),

respectively, with a transimpedance gain of $10^5\ \text{V/A}$ and a quantum efficiency of 90%. The obtained photocurrents i_1 , i_2 , and i_3 are subtracted from each other to get their subtractions $i_3 - i_2$, $i_3 - i_1$, $i_2 - i_1$, and $i_3 - i_2 - i_1$ by using two radiofrequency subtractors (S₁ and S₂). These photocurrents are analyzed using a spectrum analyzer (SA) set to a 30 kHz resolution bandwidth (RBW) and a 300 Hz video bandwidth (VBW), which gives the variances of these photocurrents.

We first record the noise power of photocurrent of $i_3 - i_2 - i_1$, which gives the intensity-difference squeezing of triple-beams (DS_{321}) after comparing with its corresponding SNL. We denote both the triple-beam intensity-difference squeezing and the pairwise correlations for the ideal case, the case with the consideration of losses and the case of the experimental results by using a superscript $k = 1, 2$, and 3, respectively, through the entire paper.

Theoretically, DS_{321} of triple-beams for the ideal case is given by

$$DS_{321}^{(1)} = 10 \lg \frac{\text{Var}(I_3 - I_2 - I_1)}{\langle I_3 + I_2 + I_1 \rangle} = 10 \lg \frac{1}{2G_1G_2 - 1}. \quad (1)$$

Taking into account transmission loss and detection loss, it becomes

$$DS_{321}^{(2)} = 10 \lg \frac{-1 + 2\eta + G_1(1 + (2G_2 - 1)\eta_{int} + \eta(-4 + 2G_1(\eta_{int} - 1)^2 - \eta_{int}(-6 + 2G_2 + \eta + \eta_{int})))}{G_1 - 1 + \eta_{int}G_1(2G_2 - 1)}. \quad (2)$$

According to Eq. (2), we can see that DS depends not only on the gain but also on the losses. So, we plot the theory curves for more than one type of loss. Figure 2(a) shows the theory curves with consideration of losses, the green one

represents the theoretical results for the case of $\eta = 0.5$ and $\eta_{int} = 0.5$, the purple one represents the theoretical results for the case of $\eta = 0.7$ and $\eta_{int} = 0.7$, the orange one represents the theoretical results for the case of $\eta = 0.9$ and $\eta_{int} = 0.93$.

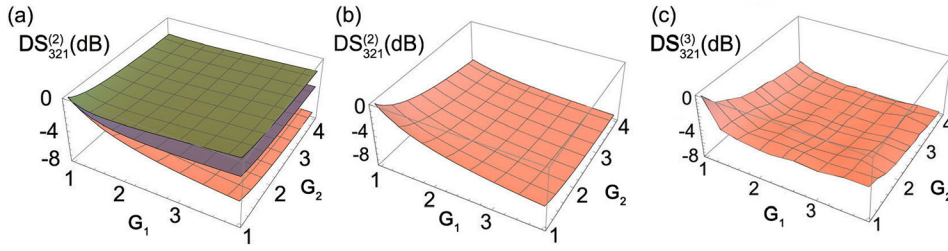


FIG. 2. The dependence of DS_{321} on G_1 and G_2 . (a) The theory curves with consideration of losses. (b) The theoretical prediction ($\eta = 0.9$ and $\eta_{int} = 0.93$). (c) The experimental results.

From Fig. 2(a), we can see that the losses can largely affect the value of the DS . According to our experimental measurement, the losses of our system are $\eta = 0.9$ and $\eta_{int} = 0.93$, and so, we study the dependence of the DS on the gain of the FWM process in this case. In order to better compare the experimental results and theoretical prediction, we separately show the theory curve for the case of $\eta = 0.9$ and $\eta_{int} = 0.93$ in Fig. 2(b). Figure 2(c) shows the experimental results of the dependence of $DS_{321}^{(3)}$ on G_1 and G_2 . It can be seen that as G_1 and G_2 increase, $DS_{321}^{(3)}$ gradually decreases, that is, the intensity-difference squeezing of triple-beams increases. This is because of the fact that although the noise power of any single beam from the quantum correlated triple-beams is amplified by the FWM process, the noise power of $i_3 - i_2 - i_1$ can return to the original noise level of Pr_0 . Such an enhancement of quantum correlation is good for the future development of a high fidelity quantum communication protocol as mentioned before. The dependence of DS_{321} on G_1 and G_2 still shows good agreement between theoretical prediction and experimental results as shown in Figs. 2(b) and 2(c).

We then investigate the pairwise intensity correlations for any pair of the triple-beams. We subtract i_2 from i_3 and record the noise power, which gives the intensity-difference squeezing (DS_{32}) of beams Pr_2 and C_2 ($i_3 - i_2$) after comparing with its corresponding SNL. PC between Pr_2 and C_2 can be quantified by

$$\begin{aligned} DS_{32}^{(1)} &= 10\lg \frac{\text{Var}(I_3 - I_2)}{\langle I_3 + I_2 \rangle} \\ &= 10\lg \frac{2G_1 - 1}{2G_2 - 1}. \end{aligned} \quad (3)$$

Similarly, the noise power spectrum of $i_3 - i_1$ gives the intensity-difference squeezing of beams Pr_2 and C_1 (DS_{31}). Therefore, PC between Pr_2 and C_1 can be quantified by

$$\begin{aligned} DS_{31}^{(1)} &= 10\lg \frac{\text{Var}(I_3 - I_1)}{\langle I_3 + I_1 \rangle} \\ &= 10\lg \frac{2G_1^2 G_2^2 - 4G_1^2 G_2 + 2G_1^2 + 3G_1 G_2 - 3G_1 + 1}{G_1 G_2 + G_1 - 1}. \end{aligned} \quad (4)$$

Along this line, PC between C_2 and C_1 can be quantified by

$$\begin{aligned} DS_{21}^{(1)} &= 10\lg \frac{\text{Var}(I_2 - I_1)}{\langle I_2 + I_1 \rangle} \\ &= 10\lg \frac{2G_1^2 G_2^2 - 8G_1^2 G_2 + 8G_1^2 + 5G_1 G_2 - 8G_1 + 1}{G_1 G_2 - 1}. \end{aligned} \quad (5)$$

Taking into account transmission loss and detection loss, the three PCs can be quantified by

$$DS_{32}^{(2)} = 10\lg \frac{-1 - 2G_2(\eta - 1) + 2\eta(1 + (G_1 - 1)\eta_{int})}{2G_2 - 1}, \quad (6)$$

$$DS_{31}^{(2)} = 10\lg \frac{2\eta - 1 + G_1(1 + \eta_{int}G_2 + 2\eta(-2 + \eta_{int}G_2(1 + G_2 - \eta_{int}G_2) + G_1(\eta_{int}G_2 - 1)^2))}{G_1 - 1 + \eta_{int}G_1G_2}, \quad (7)$$

$$DS_{21}^{(2)} = 10\lg \frac{G_1 - 1 + 2(G_1 - 1)^2\eta + (G_2 - 1)G_1(1 + 2(1 + G_2 - 2G_1)\eta)\eta_{int} + (G_2 - 1)^2G_1(2G_1 - 1)\eta_{int}^2}{G_1 - 1 + \eta_{int}G_1(G_2 - 1)}. \quad (8)$$

Figures 3(a), 3(d), and 3(g) show the theory curves with consideration of losses. The one in the same color represents the same case of losses as before, Fig. 2(a). We can see that the losses can largely affect the value of DS .

In order to generate the intensity-difference squeezing in the FWM process, we usually inject a coherent state into the system. Although the beams Pr_2 and C_2 are generated by seeding the thermal state Pr_1 into the second FWM process, they can still exhibit intensity-difference squeezing when $G_2 > G_1$. The amplified noise level of the thermal state Pr_1 is proportional to $2G_1 - 1$, and the noise level of the relative intensity difference between Pr_2 and C_2 is inversely proportional to $2G_2 - 1$. Therefore, pairwise correlation between

the beams Pr_2 and C_2 will depend on the relative value of $2G_1 - 1$ and $2G_2 - 1$. That is to say, the beams Pr_2 and C_2 show intensity-difference squeezing for $G_2 > G_1$. Otherwise, there is no intensity-difference squeezing for $G_2 \leq G_1$. Figure 3(b) shows the theoretical results of the dependence of $DS_{32}^{(2)}$ on G_1 and G_2 (for the case of $\eta = 0.9$ and $\eta_{int} = 0.93$). Figure 3(c) shows the corresponding experimental results of the dependence of $DS_{32}^{(3)}$ on G_1 and G_2 . It can be seen that the experimental results are in good agreement with the theoretical prediction.

Next, we study the dependence of DS_{31} on G_1 and G_2 . The beams Pr_1 and C_1 are the twin beams produced by the first FWM process. The beams Pr_1 and C_1 show intensity-

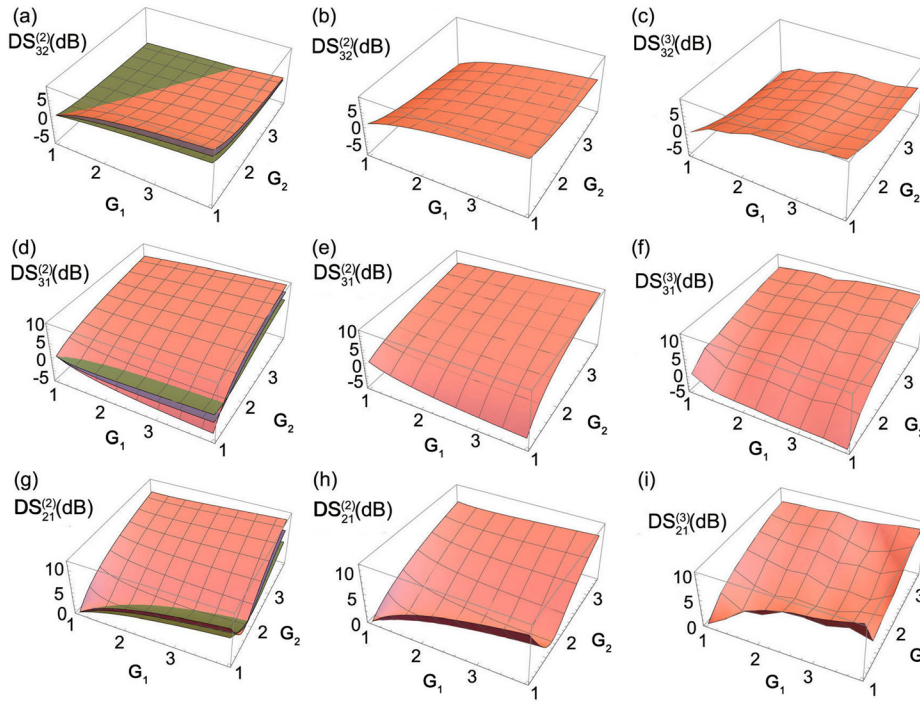


FIG. 3. The dependence of DS_{32} , DS_{31} , and DS_{21} on G_1 and G_2 . (a), (d), and (g) The theory curves with consideration of losses. (b), (e), and (h) The theoretical prediction ($\eta = 0.9$ and $\eta_{int} = 0.93$). (c), (f), and (i) The experimental results.

difference squeezing, and the intensity-difference squeezing is inversely proportional to $2G_1 - 1$. The noise of the beam Pr_1 is further amplified after the second FWM process and becomes the beam Pr_2 , and the noise level of beam Pr_2 is proportional to $2G_2 - 1$. Therefore, if the intensity-difference squeezing of the beams Pr_2 and C_1 is to be observed, the condition $G_2 \ll G_1$ should be satisfied. Such a condition is equivalent to make the first FWM dominate the whole cascaded FWM processes or make the amplification effect of the second FWM negligible. In this way, the beams Pr_2 and C_1 will share quantum correlation. Figure 3(e) shows the theoretical results of the dependence of $DS_{32}^{(2)}$ on G_1 and G_2 (for the case of $\eta = 0.9$ and $\eta_{int} = 0.93$). Figure 3(f) shows the experimental results of the dependence of $DS_{31}^{(3)}$ on G_1 and G_2 . It can be seen that the experimental results are in good agreement with the theoretical prediction.

Along this line, Fig. 3(h) shows the theoretical results of the dependence of $DS_{21}^{(2)}$ on G_1 and G_2 (for the case of $\eta = 0.9$ and $\eta_{int} = 0.93$). $DS_{21}^{(2)} \geq 0$ is always satisfied, indicating that the beams C_2 and C_1 cannot have the intensity-difference squeezing. The reason is that there is not any interaction between C_2 and C_1 during the whole cascaded FWM processes. Figure 3(i) shows the corresponding experimental

results of the dependence of $DS_{21}^{(3)}$ on G_1 and G_2 . The experimental results of the dependence of DS_{21} on G_1 and G_2 are consistent with the theoretical prediction.

Due to the fact that $DS_{21} \geq 0$ is always satisfied and shows no quantum correlation, it would be interesting to compare the two pairwise correlations DS_{32} and DS_{31} which can be possibly operated in the quantum regime. Figure 4(a) shows the theoretical prediction for both $DS_{32}^{(2)} < 0$ and $DS_{31}^{(2)} < 0$ (for the case of $\eta = 0.9$ and $\eta_{int} = 0.93$). Figure 4(b) shows the corresponding experimental results. Based on these results, it can be clearly seen that there is no overlap between DS_{32} and DS_{31} . In other words, beam Pr_2 cannot be simultaneously quantum correlated with beams C_1 and C_2 . It can be explained by the competition between the correlation mechanism and the decorrelation mechanism. As shown in Fig. 1(a), first, for the PC between beams C_1 and Pr_2 , obviously, cell₁ will provide the correlation between them and cell₂ will destroy their quantum correlation by adding extra vacuum noise, and thus, cell₁ and cell₂ can be viewed as the correlation mechanism provider and the decorrelation mechanism provider respectively; thus, we can increase G_1 and decrease G_2 to enhance the PC between beams Pr_2 and C_1 . Second, for the case of the PC between beams Pr_2 and C_2 ,

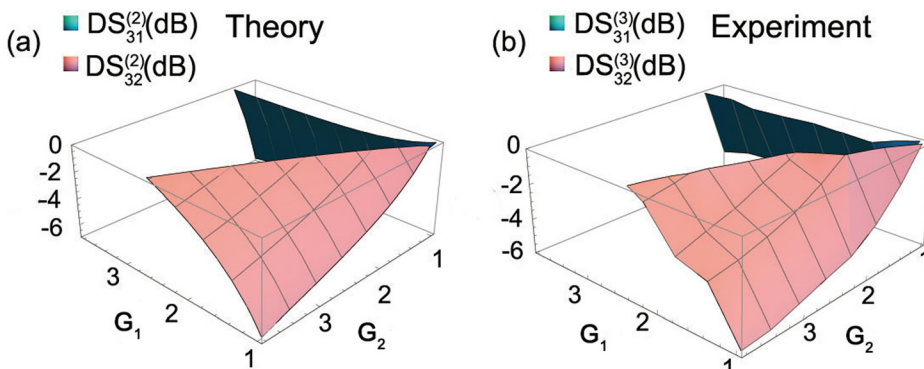


FIG. 4. Comparison of quantum pairwise correlations DS_{32} and DS_{31} . (a) The theoretical prediction ($\eta = 0.9$ and $\eta_{int} = 0.93$). (b) The experimental results.

cell₁ will generate a thermal state Pr_2 which will destroy their quantum correlation by adding extra vacuum noise into the system, while cell₂ will make them quantum correlated through the FWM process. In this case, cell₁ and cell₂ can be viewed as the decorrelation mechanism provider and the correlation mechanism provider, respectively, and thus, we can decrease G_1 and increase G_2 to enhance the PC between beams Pr_2 and C_2 . Finally, the complete opposite dependence of the PC between beams C_1 and Pr_2 and the PC between beams Pr_2 and C_2 on the gains leads to the non-overlapping between DS_{32} and DS_{31} . Such a phenomenon may be useful for quantum secret sharing networks, in which the three generated beams from our cascaded FWM process are the three nodes of the quantum network, respectively. The pairwise correlation of any pair of the three beams is the edges of the quantum network. Our results show that the pairwise correlations can be manipulated by tuning the gains of the cascaded FWM process. As a result, the three nodes are hierarchical. Among them, node Pr_2 can be quantum correlated with the other two nodes C_2 and C_1 , respectively, but cannot be quantum correlated with them at the same time. The other two nodes C_2 and C_1 cannot be quantum correlated with each other. In some gain region, all the three pairwise correlations are in the classical regime without any quantum correlation. These results are mainly due to the asymmetric structure of our cascaded FWM processes, which directly leads to the asymmetric roles of the generated three beams. Such unbalanced and controllable pairwise correlations are actually useful for secure quantum communication in which participants should have different levels of authorities for secure purposes. In this sense, such unbalanced and controllable pairwise correlation structures may be taken as advantages in practical quantum communications, for example, hierarchical quantum secret sharing.

In conclusion, we have theoretically characterized and experimentally measured the performance of the pairwise correlations from the triple quantum correlated beams and analyzed the dependence of all the PCs on the system intensity gains based on two different cascaded FWM processes. The cascaded FWM process produces triple-beams which can always remain in the quantum regime ($DS_{321} < 0$ is always satisfied). However, the PC of any pair of the triple-beams is not always in the quantum regime. We have found that two of them (Pr_2 and C_2 ; Pr_2 and C_1) can be transformed from the classical regime to the quantum regime by changing the system intensity gains. More interestingly, their quantum regions of system intensity gains are not overlapped. The PC of beams C_1 and C_2 is always in the classical regime, showing that there is no quantum correlation between C_1 and C_2 for the whole gain regions. Our results open the way for the classification and application of quantum states generated from the cascaded FWM processes.

This work was supported by the National Natural Science Foundation of China (NSFC) (91436211, 11374104, and 10974057); Natural Science Foundation of Shanghai (17R1442900); The program of scientific and technological innovation of Shanghai (17JC1400401); National Basic Research Program of China (2016YFA0302103); SRFDP (20130076110011); and Program of Introducing Talents of Discipline to Universities (B12024).

- ¹A. Einstein, B. Podolsky, and N. Rosen, *Phys. Rev.* **47**, 777 (1935).
- ²D. M. Greenberger, M. A. Horne, and A. Zeilinger, *Phys. Today* **46**(8), 22 (1993).
- ³C. Weedbrook, S. Pirandola, R. G. Patr, N. J. Cerf, T. C. Ralph, J. H. Shapiro, and S. Lloyd, *Rev. Mod. Phys.* **84**, 621 (2012).
- ⁴H. J. Kimble, *Nature* **453**, 1023–1030 (2008).
- ⁵S. L. Braunstein and P. V. Loock, *Rev. Mod. Phys.* **77**, 513–577 (2005).
- ⁶M. D. Lukin, *Rev. Mod. Phys.* **75**, 457 (2003).
- ⁷E. Schneidman, S. Still, M. J. Berry II, and W. Bialek, *Phys. Rev. Lett.* **91**, 238701 (2003).
- ⁸K. Shimizu and D. Hashimoto, *Phys. Rev. A* **79**, 062312 (2009).
- ⁹V. Coffman, J. Kundu, and W. K. Wootters, *Phys. Rev. A* **61**, 052306 (2000).
- ¹⁰L. Amico, R. Fazio, A. Osterloh, and V. Vedral, *Rev. Mod. Phys.* **80**, 517–576 (2008).
- ¹¹L. Borsten, D. Dahanayake, M. J. Duff, W. Rubens, and H. Ebrahim, *Phys. Rev. A* **80**, 032326 (2009).
- ¹²A. Acn, D. Bru, A. Lewenstein, and A. Sanpera, *Phys. Rev. Lett.* **87**, 040401 (2001).
- ¹³L. Borsten, D. Dahanayake, M. J. Duff, A. Marrani, and W. Rubens, *Phys. Rev. Lett.* **105**, 100507 (2010).
- ¹⁴G. Rigolin, T. R. de Oliveira, and M. C. de Oliveira, *Phys. Rev. A* **74**, 022314 (2006).
- ¹⁵U. Vogl, R. T. Glasser, and P. D. Lett, *Phys. Rev. A* **86**, 031806(R) (2012).
- ¹⁶Z. Qin, L. Cao, and J. Jing, *Appl. Phys. Lett.* **106**, 211104 (2015).
- ¹⁷Z. Zhang, F. Wen, J. Che, D. Zhang, C. Li, Y. Zhang, and M. Xiao, *Sci. Rep.* **5**, 15058 (2015).
- ¹⁸B. J. Lawrie, P. G. Evans, and R. C. Pooser, *Phys. Rev. Lett.* **110**, 156802 (2013).
- ¹⁹A. M. Marino, V. Boyer, R. C. Pooser, P. D. Lett, K. Lemons, and K. M. Jones, *Phys. Rev. Lett.* **101**, 093602 (2008).
- ²⁰C. Liu, J. Jing, Z. Zhou, R. C. Pooser, F. Hudelist, L. Zhou, and W. Zhang, *Opt. Lett.* **36**, 2979–2981 (2011).
- ²¹C. F. McCormick, V. Boyer, E. Arimondo, and P. D. Lett, *Opt. Lett.* **32**, 178–180 (2007).
- ²²L. Cao, J. Qi, J. Du, and J. Jing, *Phys. Rev. A* **95**, 023803 (2017).
- ²³Y. Cai, J. Feng, H. Wang, G. Ferrini, X. Xu, J. Jing, and N. Treps, *Phys. Rev. A* **91**, 013843 (2015).
- ²⁴A. M. Marino, R. C. Pooser, V. Boyer, and P. D. Lett, *Nature* **457**, 859–862 (2009).
- ²⁵V. Boyer, A. M. Marino, R. C. Pooser, and P. D. Lett, *Science* **321**, 544–547 (2008).
- ²⁶R. C. Pooser and B. Lawrie, *Optica* **2**, 393–399 (2015).
- ²⁷C. S. Embrey, M. T. Turnbull, P. G. Petrov, and V. Boyer, *Phys. Rev. X* **5**, 031004 (2015).
- ²⁸J. Jing, C. Liu, Z. Zhou, Z. Y. Ou, and W. Zhang, *Appl. Phys. Lett.* **99**, 011110 (2011).
- ²⁹H. Chen, M. Qin, Y. Zhang, X. Zhang, F. Wen, J. Wen, and Y. Zhang, *Laser Phys. Lett.* **11**, 045201 (2014).
- ³⁰C. Li, Z. Jiang, Y. Zhang, Z. Zhang, F. Wen, H. Chen, Y. Zhang, and M. Xiao, *Phys. Rev. Appl.* **7**, 014023 (2017).
- ³¹Z. Qin, L. Cao, H. Wang, A. M. Marino, W. Zhang, and J. Jing, *Phys. Rev. Lett.* **113**, 023602 (2014).